

# SiN<sub>x</sub>/SiO<sub>2</sub> STACKED SENSITIVE THIN FILM FOR ISFET-BASED CHEMICAL AND BIOCHEMICAL SENSORS

## *Preparation and Characterization of the Stacked Thin Films and Sensors*

J. F. Souza<sup>1,2,3</sup>, M. B. Lima<sup>4</sup>, I. Doi<sup>1,2</sup>, P. J. Tatsch<sup>1,2</sup>, J. A. Diniz<sup>1,2</sup> and J. L. Gonçalves<sup>3</sup>

<sup>1</sup>School of Electrical and Computer Engineering, University of Campinas, Av. Albert Einstein 400, Campinas, SP, Brazil

<sup>2</sup>Center for Semiconductor Components, University of Campinas, R. João Pandiá Calógeras 90, Campinas, SP, Brazil

<sup>3</sup>Center for Information Technology Renato Archer, Rod. D. Pedro I (SP – 65) Km 143, 6, Campinas, SP, Brazil

<sup>4</sup>Superior School of Sciences of the Health, University of Amazonas, Av. Carvalho Leal, 1777, Manaus, AM, Brazil

**Keywords:** SiN<sub>x</sub>/SiO<sub>2</sub>, Silicon nitride thin film, ISFET, Chemical sensor, Biochemical sensor.

**Abstract:** In this work, nitrogen rich SiN<sub>x</sub> thin film was deposited on SiO<sub>2</sub>/p-Si (100) substrate by low pressure chemical vapour deposition (LPCVD). The film was physically characterized using techniques such as Fourier transform infrared spectroscopy (FTIR), atomic force microscopy (AFM) and ellipsometry. The biocompatibility of such film was investigated by FTIR. Using a set of metal insulator semiconductor field effect transistors (MISFETs) and ion sensitive field effect transistors (ISFETs) fabricated, electrical characteristics and sensing properties were investigated. The biocompatibility of the SiN<sub>x</sub> film and the electrical quality of the SiN<sub>x</sub>/SiO<sub>2</sub>/p-Si interface obtained suggests that SiN<sub>x</sub>/SiO<sub>2</sub> is an adequate insulator on ISFET based chemical and biochemical sensors.

## 1 INTRODUCTION

LPCVD Si<sub>3</sub>N<sub>4</sub> films are used as the sensitive material in miniaturized ISFET-based chemical and biochemical sensors. Such devices have been used for example for further surface modifications allowing for antigen-antibody biosensor applications. In vivo studies classify Si<sub>3</sub>N<sub>4</sub> as a biocompatible material (Gustavsson et al., 2008). The first ISFET was applied by Bergveld (Bergveld, 1970) to a biosensor for measuring ion concentration in nerve tissues. The latest investigations related to the ISFET-based biosensor are extended to immunosensing (Schenck, 1978, Schöning and Poghossian, 2002) and DNA hybridization sensing (Souteyrand et al., 1997, Pouthas et al., 2004). Ultrasensitive detection of biomolecules using various types of one-dimensional nanostructures such as carbon nanotubes (Villamizar et al., 2008), graphenes (Cheng et al., 2010) and nanowires (Knopfmacher et al., 2010) has attracted broad research interest during the past decade due to their high surface-to-volume ratio. An important parameter, the slope of characteristic, is directly related with sensitivity of the sensor. These aspects

have not been yet convincingly reported, for this reason, this work reports the use of SiN<sub>x</sub>/SiO<sub>2</sub> stacked sensitive thin films that are biocompatible and present high quality of the electrical interface, increasing the sensitivity and making possible a direct electrical detection of charged molecules.

## 2 EXPERIMENTS

### 2.1 SiN<sub>x</sub>/SiO<sub>2</sub> Stacked Sensitive Thin Film Preparation

The (100)-orientated 1-10 Ω.cm p-type silicon wafers were used as substrates. The 5 nm thick thermally grown silicon oxide (SiO<sub>2</sub>) film was prepared using a conventional furnace at 1000 °C for 1 minute, in a high purity oxygen atmosphere. Then, the SiN<sub>x</sub> layer, a sensing membrane, was deposited by LPCVD in a SiCl<sub>2</sub>H<sub>2</sub>/NH<sub>3</sub> gas mixture atmosphere at 740 °C. The base and work pressure of the chamber were 10 mTorr and 0.57 Torr, respectively. The flow rate of SiCl<sub>2</sub>H<sub>2</sub> was fixed at 23 standard cubic centimeters per minute (sccm), while the flow rate of NH<sub>3</sub> was 60 sccm. All

deposition parameters are shown in Table 1.

Table 1: Parameters for the deposition of SiN<sub>x</sub> film.

SiCl <sub>2</sub> H <sub>2</sub> flow rate	23 sccm
NH <sub>3</sub> flow rate	60 sccm
Temperature of the substrate	740 °C
Base pressure	10 mTorr
Work pressure	0.57 Torr
Deposition rate	27 Å/min

## 2.2 Immunoglobulin's Self-assembled Monolayer (SAM) Preparation

Figure 1 shows a schematic diagram of the method used to prepare the substrates (functionalization). The substrates were cleaned using a standard RCA wet process. The 3-Aminopropyltriethoxysilane (APTS) coating was carried out in a solution of 5% APTS in toluene for 6 h, at 80 °C. The non-adsorbed APTS was removed by rinsing the substrate with toluene and ethanol and dried with N<sub>2</sub> gas. The APTS-modified substrates were baked in an oven at 110 °C for 16 h. To form the immunoglobulin's SAM (Figure 1, immobilization), the substrates coated with APTS were immersed into a solution of ethylcarbodiimide (EDC), 2 mM, N-hydroxysuccinimide (NHS), 5 mM, and immunoglobulin - IgG, 1 µg/ml, at room temperature for 2 h, and then washed with phosphate buffered saline (PBS) of pH 7.2 and deionized water (18 MΩ).

## 2.3 MISFET and ISFET Structures Fabrication

For the MISFET and ISFET the SiN<sub>x</sub>/SiO<sub>2</sub> stacked sensitive thin film were used as gate dielectric on p-type (1-10 Ω.cm) Si (100) substrate. The substrates were cleaned using a standard RCA wet process. The critical steps in this fabrication procedure are as follow:

- 1) Thermal gate oxide: 50 Å;
- 2) SiN<sub>x</sub> deposition by LPCVD: 300 Å;
- 3) SiN<sub>x</sub> dry etching and oxide wet etching of the source and drain regions;
- 4) Al etching of gate electrode; and
- 5) Entire device coated with insulating layer to eliminate ionic short circuits due to exposure to solutions.

## 2.4 SiN<sub>x</sub> Layer Characterizations

The SiN<sub>x</sub> thin films used in these studies were

characterized by FTIR (infrared spectra with 32 scans and 4 cm<sup>-1</sup> resolution), AFM in contact image mode (surface morphology), and ellipsometry (film thickness and refractive index).

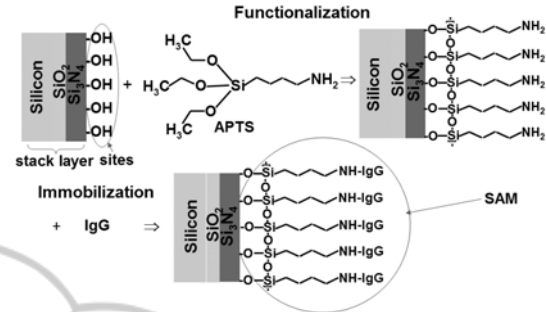


Figure 1: Schematic diagram of the preparation of the substrates (functionalization) and formation of the immunoglobulin's SAM (immobilization).

## 2.5 IgG's SAM Characterization

After immunoglobulin's SAM preparation, Fourier transform infrared spectra were performed. All spectra are collected with 32 scans and 4 cm<sup>-1</sup> resolution.

## 2.6 Measurements Setup

In order to study electrical and sensing properties, current-voltage ( $I_{DS}$ - $V_{GS}$ ) and current-time ( $I_{DS}$ -time) of MISFETs and ISFETs structures were measured by a semiconductor parameter analyzer Keithley 4200-SCS. The gate voltages were applied to an aluminium metal gate of MISFETs and a gold reference electrode for ISFETs.

# 3 RESULTS AND DISCUSSION

## 3.1 Physical Characteristics of SiN<sub>x</sub> Film

The FTIR spectrum of SiN<sub>x</sub> (Figure 2) exhibits a clearly pronounced peak at 828 cm<sup>-1</sup> and smaller peak at 467 cm<sup>-1</sup>, which are typical for the Si-N bond in amorphous silicon nitride (Beshkov et al., 2003). The deposition rate is 27 Å/min and the films have high refractive index  $n = 2.0$  indicating that the films are nitrogen rich. The AFM image (Figure 3) shows the formation of very smooth and uniform SiN<sub>x</sub> films, with average (Ra) and root mean square (Rrms) roughness of 0.31 nm and 0.46 nm, respectively.

### 3.2 IgG's SAM Characteristics

The characteristic vibrational peaks are mainly dominated by the protein constituents of the IgG's SAM (Figure 4). A vibration band assignment is done with the idea of the group frequencies of the various analytes present in the SAM. The spectral region  $3600\text{--}3000\text{ cm}^{-1}$  comprises of C-H, O-H, and N-H stretching vibrations of the proteins. The prominent absorption peak at  $3300\text{ cm}^{-1}$  is due to the N-H stretching mode (amide A) of proteins. The asymmetric and symmetric stretching C-H vibrations of methyl and methylene group are found to be present around  $2930\text{--}2875\text{ cm}^{-1}$ . The strong absorption band at  $1650\text{ cm}^{-1}$  correspond to C=O stretching vibrations (amide I) whereas the vibration band at  $1542\text{ cm}^{-1}$  is attributed as amide II arising of N-H bending vibrations strongly coupled with C-N stretching of proteins. The absorption peaks in the region  $1400\text{--}1200\text{ cm}^{-1}$  arise due to the C-H deformation of methyl and methylene group of the proteins. The spectral region  $1250\text{--}925\text{ cm}^{-1}$  is predominantly occupied by C-O-C asymmetric and symmetric vibrations of phospholipids of proteins (Sankari et al., 2010).

### 3.3 Electrical Properties of Devices

**MISFET** – Electrical characteristics of MISFETs including transconductance ( $G_m$ ), current-off ( $I_{off}$ ) and subthreshold swing ( $S_t$ ) were calculated through drain-source current versus gate-source voltage ( $I_{DS}\text{--}V_{GS}$ ) curves of the stack  $\text{SiN}_x/\text{SiO}_2$  gate MISFET (Figure 5). The  $I_{off}$  extracted at  $V_{GS}=V_T - 0.5\text{ V}$  was  $2.17 \times 10^{-10}\text{ A}$ . The calculated maximum transconductance of the stack  $\text{SiN}_x/\text{SiO}_2$  gate MISFET was  $1.4\text{ }\mu\text{S}$ .  $S_t$  is the slope of  $V_{GS}$  versus  $\log I_{DS}$ . The  $S_t$  was obtained from the inverse of slope in subthreshold region and is  $147\text{ mV/dec}$  to the stack  $\text{SiN}_x/\text{SiO}_2$  gate MISFET. These values are acceptable for FET operation in an analog readout circuit.

**SENSING PROPERTIES** – For pH sensitivity calculation of the stack  $\text{SiN}_x/\text{SiO}_2$  gate ISFET, the  $I_{DS}$  vs.  $V_{GS}$ ,  $I_{DS}$  vs.  $V_{DS}$  and  $I_{DS}$  vs. time curves in saturation region were measured in standard pH buffer solutions (pH 4, 7 and 10) at room temperature. In Figure 6, the obvious linear shift of  $I_{DS}\text{--}V_{GS}$  curves in different pH buffer solutions were shown. The pH response and sensitivity was  $50\text{ mV/pH}$  ( $I_{DS}=5\text{ }\mu\text{A}$ ), so a quasi-Nernstian response.

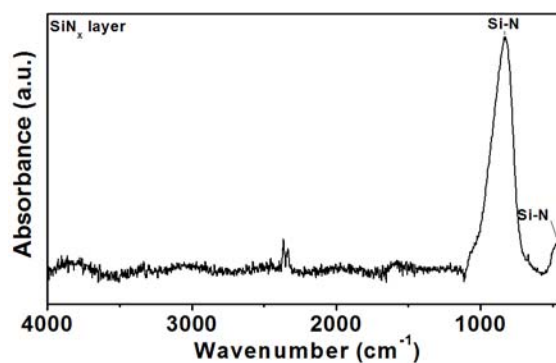


Figure 2: FTIR spectrum of  $\text{SiN}_x$  film deposited in LPCVD reactor at  $740\text{ }^\circ\text{C}$  with  $\text{SiCl}_2\text{H}_2$  and  $\text{NH}_3$ .

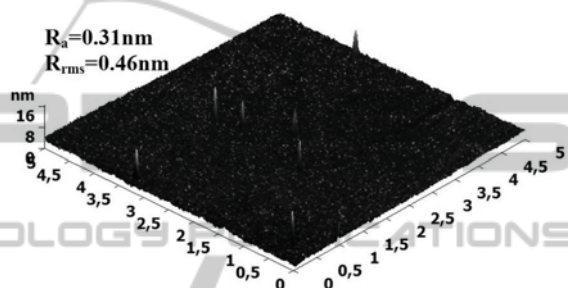


Figure 3: Surface morphology of  $\text{SiN}_x$  film on  $\text{SiO}_2$ .

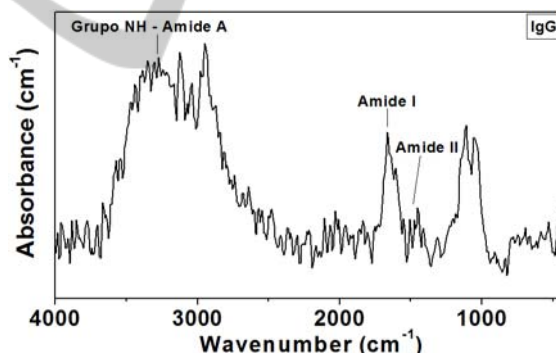


Figure 4: FTIR spectrum of immunoglobulin's SAM.

The behaviour of current in function of time was measured at constant drain-source and gate-source voltage ( $V_{DS}=V_{GS}=2\text{ V}$ ). As can be seen in Figure 7 and 8, the device showed an increase in current when the pH value was increased. The pH sensibility was  $1.24\text{ }\mu\text{A/pH}$ . The linearity of the stack  $\text{SiN}_x/\text{SiO}_2$  gate ISFET response is 97.4% in voltage mode and 99.4% in current mode. Therefore, both the pH responses are excellent in linearity. The characteristic curves of the stack  $\text{SiN}_x/\text{SiO}_2$  gate ISFET shows the normal FET operation and exhibit the similar electrical characteristics as MISFETs.

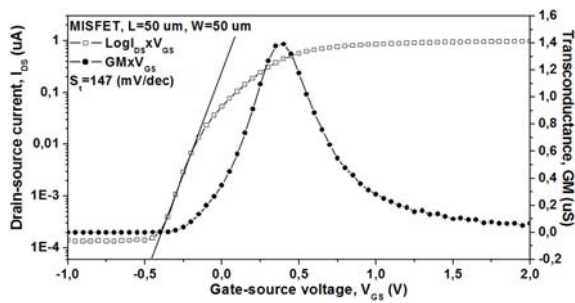


Figure 5: Log  $I_{DS}$  vs.  $V_{GS}$  and  $G_m$  vs.  $V_{GS}$  characteristics of the stack  $\text{SiN}_x/\text{SiO}_2$  gate MISFET.

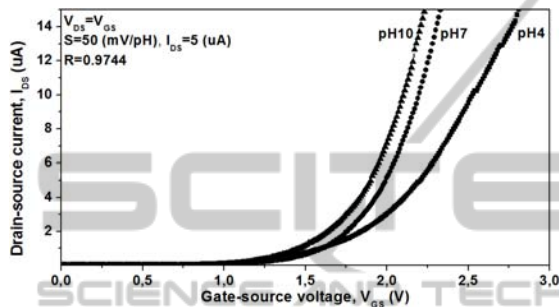


Figure 6:  $I_{DS}$  vs.  $V_{GS}$  curves of the stack  $\text{SiN}_x/\text{SiO}_2$  gate ISFET measured at room temperature in standard pH buffer solutions (pH 4, 7 and 10).

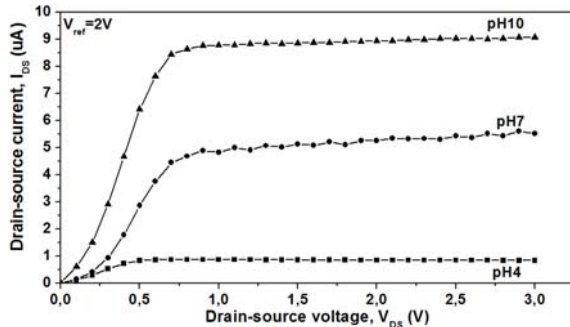


Figure 7:  $I_{DS}$  vs.  $V_{DS}$  curves of the stack  $\text{SiN}_x/\text{SiO}_2$  gate ISFET measured at room temperature in standard pH buffer solutions (pH 4, 7 and 10).

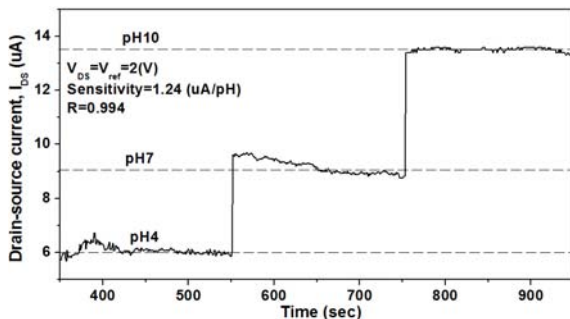


Figure 8:  $I_{DS}$  vs. time curve in saturation region, measured in standard pH buffer solutions (pH 4, 7 and 10) at room temperature ( $V_{DS} = V_{GS} = 2V$ ).

## 4 CONCLUSIONS

In this study, stacked sensing membrane with LPCVD  $\text{SiN}_x$  on  $\text{SiO}_2$  was used for ISFET-based chemical and biochemical sensors. The  $\text{SiN}_x$  obtained was very smooth and nitrogen rich. By fabricating and characterizing Immunoglobulin's self assembled monolayer we have demonstrated the biocompatibility of the films. Electrical and sensing properties were investigated by means of the stack  $\text{SiN}_x/\text{SiO}_2$  gate MISFETs and ISFETs, respectively. The results showed that the MISFET exhibits good electrical characteristics. In regard to pH sensing properties analysis, the stack  $\text{SiN}_x/\text{SiO}_2$  ISFET-based sensor presented high performance with almost Nernstian response (sensitivity of 50 mV/pH) and high linearity of 97.4% in voltage mode and 99.4% in current mode. The obtained results demonstrate therefore the feasibility of ISFET-based sensors for the detection of charged molecules.

## ACKNOWLEDGEMENTS

The authors would like to thanks the CCS staff for technical assistance and the Brazilian agencies CNPq, CAPES, FAPESP, and INCT-NAMITEC for the financial support.

## REFERENCES

- Gustavsson, J., Altankov, G., Errachid, A., Samitier, J., Planell, J. A., Engel, E. (2008). Surface modifications of silicon nitride for cellular biosensor applications. *J. Mater Sci: Mater Med*, 19, 1839–1850.
- Bergveld, P. (1970). Development of an Ion-Sensitive Solid-State Device for Neurophysiological Measurements. *IEEE Transactions on bio-medical engineering*, 17, 70–71.
- Schenck, J. F. (1978). In Cheung, P.W. (Ed.), *Theory Design and Biomedical Applications of Solid State Chemical Sensors* (pp. 165–173). CRC Press: Boca Raton.
- Schöning, M. J., Poghossian, A. (2002). Recent advances in biologically sensitive field-effect transistors (BioFETs). *Analyst*, 127, 1137–1151.
- Souteyrand, E., Colarec, J. P., Martin, J. R., Wilson, C., Lawrence, I., Mikkelsen, S., Lawrence, M. F. (1997). Direct Detection of the Hybridization of Synthetic Homo-Oligomer DNA Sequences by Field Effect. *J. Phys. Chem. B*, 101, 2980–2985.
- Pouthas, F., Gentil, C., Côte, D., Bockelmann, U. (2004). U. DNA detection on transistor arrays following mutation-specific enzymatic amplification. *Appl. Phys. Lett.*, 84, 1594–1596.

- Villamizar, R. A., Maroto, A., Rius F. X., Inza, I., Figueras, M. J. (2008). Fast detection of Salmonella Infantis with carbon nanotube field effect transistors. *Biosensors and Bioelectronics*, 24, 279–283.
- Cheng, Z., Li, Q., Li, Z., Zhou, Q., Fang, Y. (2010). Suspended Graphene Sensors with Improved Signal and Reduced Noise. *Nano Lett.*, 10, 1864–1868.
- Knopfmacher, O., Tarasov, A., Fu, W., Wipf, M., Niesen, B., Calame, M., Schönenberger, C. (2010). Nernst Limit in Dual-Gated Si-Nanowire FET Sensors. *Nano Lett.*, 10, 2268–2274.
- Beshkov G., Lei S., Lazarova V., Nedev N., Georgiev S. S. (2003). IR and Raman absorption spectroscopic studies of APCVD, LPCVD and PECVD thin SiN films. *Vacuum*, 69, 301–305.
- Sankari G., Krishnamoorthy E., Jayakumaran S., Gunasekaran S., Priya V. V., Subramaniam S., Mohan S. K. (2010). Analysis of serum immunoglobulins using Fourier transform infrared spectral measurements. *Biology and Medicine*, 2 (3), 42–48.

